Organic Process Research & Development **1999**, *3*, 404−408

Development of the Process of *p*-Nitroacetophenone and Benzoic Acid Manufacture by the Liquid-Phase Oxidation of Aromatic Compounds

Tatiana V. Bukharkina,* Nikolai G. Digurov, Sergey B. Mil'ko, and Anna B. Shelud'ko

D.I. Mendeleev University of Chemical Technology of Russia, 9 Miusskaya sq., Moscow, 125047, Russia

Abstract:

The kinetic model of the ethyl benzene oxidation was applied to the design of the large-scale reactors of *p*-nitroacetophenone (chloramphenicol key intermediate) synthesis by *p*-nitroethyl benzene oxidation and benzoic acid synthesis by acetophenone oxidation. The factors allowing simplification of the above model are discussed. The height of the frothy (aerated) liquid layer in the oxidation tower securing the explosion-proof reaction conditions of acetophenone and *p*-nitroethyl benzene oxidation both in the kinetic and diffusion fields was calculated.

The oxygen-containing ethyl benzene derivatives are frequently used in industry either as intermediates or the final products. In some cases their manufacture by the liquid-phase catalytic oxidation by gaseous oxygen is quite promising. The syntheses of benzoic acid (BA) from acetophenone (AP) (eq 1) and *p*-nitroacetophenone (p-NAP) from *p*-nitroethyl benzene (p-NEB) (eq 2) are examples of such processes.

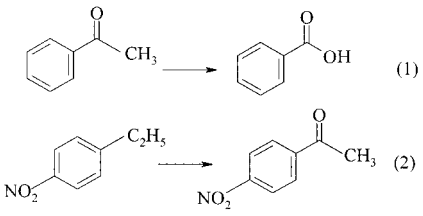

Acetophenone is a side-product of the Halcon process and is formed in the epoxidation of styrene by ethyl benzene hydroperoxide. Acetophenone can be used for the production of benzoic acid applied as an agricultural foodstuff preservative and an organic synthesis intermediate. *p*-Nitroacetophenone is a starting product in the chloramphenicol and synthomycin syntheses.

The commercialisaton of these processes either on a pilot- or on a large-scale requires the solution of the chemical problems (the choice of the optimal reaction conditions) as well as the engineering ones (the choice of explosion-proof equipment capable of providing the effective mixing, the isolation of products, the recycling of the unreacted reagents, etc.). In this work we intend to demonstrate how the data obtained in the study of the EB oxidation were applied to the solution of the above-mentioned tasks.

* Author for correspondence. Fax: +7 (095) 973 3136. E-mail: kra@muctr.edu.ru.

Experimental Section

The experimental procedure was described earlier.[1] All of the oxidation experiments were run in a stirred batch reactor. The kinetic region was established by the independence of the reaction rate on the stirring intensity and the gas velocity at both the maximal temperature and reagent concentrations.

Results and Discussion

Kinetics of Acetophenone Oxidation to Benzoic Acid. The kinetic model of the acetophenone oxidation was proposed in the previous paper.[2] The overall form of the kinetic equation and all of the constants were obtained when pure oxygen was the oxidant, whereas in the industry this role is played by the air. The oxygen concentration can vary both in time and along the length of the reactor. Thus, it was necessary to establish the dependence of the reaction rate upon the oxygen concentration in the gas phase. The change in the oxygen concentration did not change the form of the rate equation. The effective rate constant was linearly dependent upon C_{O_2} in the range 0.05−0.21 volume fractions. It allowed us to obtain the following rate equation:

$$\frac{d[AP]}{d\tau} = -k[Mn^{3+}]C_{O_2}\frac{K[AP]/[BA]}{1 + K[AP]/[BA]} \qquad (3)$$

where $k = 0.22 \exp(-1100/T)$ min^{-1} and $K = 3.1 \pm 0.8$.

This equation can be used for the calculation of the benzoic acid synthesis reactor that works in the kinetic region.

Kinetics of *p*-NEB Oxidation to *p*-NAP. *p*-NEB is a structural analogue of EB, and thus it is reasonable to assume that they have a common oxidation mechanism. In this case the following sequence of main oxidation products formation can be envisaged as follows:

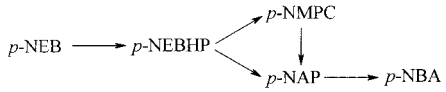

where *p*-NEB is *p*-nitroethyl benzene, *p*-NEBHP is *p*-nitroethyl benzene hydroperoxide, *p*-MNPC is methyl *p*-nitrophenyl carbinol, *p*-NAP is *p*-nitroacetophenone, and *p*-NBA is *p*-nitrobenzoic acid.

It is evident that the desired product (*p*-NAP) is the oxidation intermediate. Thus it is necessary to determine the

(1) Bukharkina, T. V.; Grechishkina, O. S.; Digurov, N. G.; Krukovskaya, N. V. *Org. Process Res. Dev.* **1999**, *3*, 400−403.
(2) Bukharkina, T. V.; Grechishkina, O. S.; Digurov, N. G.; Krukovskaya, N. V. *Org. Process Res. Dev.*, in press.

 10.1021/op990030q CCC: $18.00
Published on Web 09/23/1999

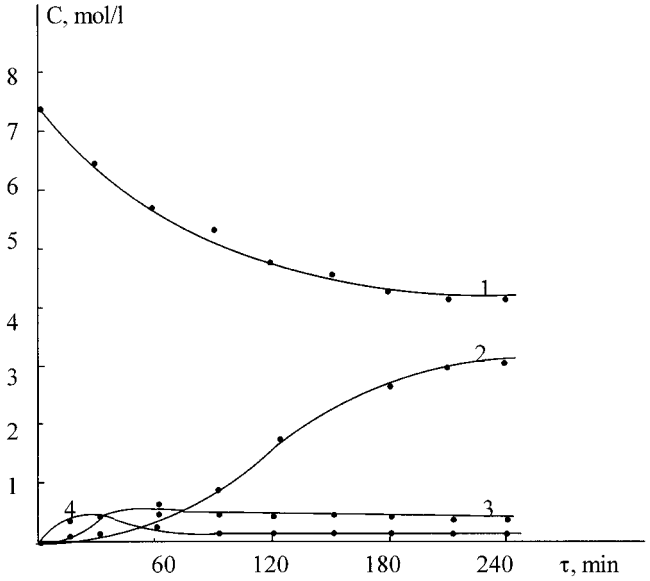

Figure 1. **The *p*-NEB oxidation without a solvent at 140 °C. [$Mn(CH_3COO)_2$] = 0.0025 M. (1) *p*-NEB, (2) *p*-NAP, (3) *p*-NMPC, (4) *p*-NEBHP.**

conditions when the rate of the ketone oxidation would be the lowest. It is known that the ratio of the rates of the hydrocarbon and ketone oxidation strongly depends on the catalyst. Thus, cobalt-containing catalysts are active in the hydrocarbon and alcohol oxidation and virtually do not catalyse the ketone oxidation, whereas manganese-containing catalysts act just the opposite. So, it was thought that cobalt-containing catalysts would secure the high fractional yield of the ketone. The reaction was carried out at 140 °C using air as the oxidant gas. Indeed, *p*-NAP was the final reaction product, only traces of *p*-NBA were present, and concentrations of the intermediates (*p*-NMPC and *p*-nitroethyl benzene hydroperoxide) were negligible. Nevertheless, the conversion of *p*-NEB after 2−2.5 h did not exceed 20−21%. The reaction was inhibited due to the excessive tar formation, and the recovery of the unreacted products was impossible. Thus, the cobalt-containing catalysts appeared inefficient in this reaction.

The experiments on ethyl benzene oxidation in the presence of the manganese catalyst[1,2] showed that the rate of the hydrocarbon consumption (the chain propagation rate) is 1.5−2 orders of magnitude higher than the rate of the ketone oxidation (the initiation rate). Consequently, even in the presence of the manganese catalyst the fractional yield of *p*-NAP should be high enough also at the high *p*-NEB conversion. All further experiments on the *p*-NEB oxidation were run in the presence of $Mn(OAc)_2$.

The oxidation kinetics were studied at 140 °C, the catalyst concentration was varied in the range 0.001−0.01 M. The *p*-NEB conversion at $[Mn(OAc)_2]_0$ = 0.025−0.01 M was 48−50%, and no tar formation was observed. The main reaction products were *p*-NAP and *p*-MNPC, and the *p*-NEBHP concentration passed through the maximum lowering to trace amounts at the end of the reaction. The *p*-NBA concentration did not exceed 5−7% of *p*-NAP (see Figure 1). The overall fractional yield of *p*-NAP in the air *p*-NEB oxidation is 82 ± 1%. The rate of *p*-NEB oxidation depends on the initial manganese acetate concentration and the oxygen concentration in the oxidant gas. Both of these dependencies are expressed by the linear-fractional functions. The reaction products also affect the reaction rate; the addition of *p*-MNPC inhibits the reaction and that of *p*-NAP somewhat increases the rate and neutralises the *p*-MNPC inhibiting effect. The addition of *p*-NEBHP and *p*-NBA in the amounts comparable to those observed in the reaction did not affect the rate. Thus, all of the effects are analogous to those observed during the "stationary" ethyl benzene oxidation.[1,2] The only differences are the absence of both the induction time and of the catalyst poisoning. This is evidently caused by the fast $Mn^{2+} \rightarrow Mn^{3+}$ transition. The reaction retardation is possibly the result of the reversible formation of the catalyst-product complex.

The kinetics of *p*-NEB oxidation is described by the same system of equations that was proposed for the second step of the ethyl benzene oxidation[2] (after induction time) with slightly different parameters. Thus, the rate equation is

$$\frac{\mathrm{d}[p\text{-NEB}]}{\mathrm{d}\tau} = -k_{1.1}[p\text{-NEB}]\sqrt{\frac{k_{3.2}C_{\mathrm{Mn(3+)}}[p\text{-NAP}]}{k_{1.3}([p\text{-NAP}] + k_{3.1}[p\text{-NMPC}])}} \quad (4)$$

The decrease in Mn^{3+} concentration during the reaction is compensated for by the increase in the *p*-NAP concentration at nearly constant alcohol concentration (see Figure 1). Thus, for all practical purposes this model can be approximated by the first-order rate equation that is valid until 35−40% *p*-NEB conversion. Then the eq 4 can be written as follows:

$$\frac{\mathrm{d}[p\text{-NEB}]}{\mathrm{d}\tau} = -k[p\text{-NEB}] \quad (5)$$

where

$$k = k_{1.1}\sqrt{\frac{k_{3.2}C_{\mathrm{Mn(3+)}}[p\text{-NAP}]}{k_{1.3}([p\text{-NAP}] + k_{3.1}[p\text{-NMPC}])}}$$

Experiments on the *p*-NEB oxidation showed that the rate constant k depends on the oxygen concentration in the oxidant gas, and the reaction rate is expressed by the equation

$$\frac{\mathrm{d}[p\text{-NEB}]}{\mathrm{d}\tau} = -k_{\mathrm{ef}}[p\text{-NEB}]\sqrt{C_{\mathrm{O_2}}} \quad (6)$$

where $k_{\mathrm{ef}} = 0.0857\ \mathrm{min}^{-1}$ is the effective rate constant and $C_{\mathrm{O_2}}$ is the volume fraction of oxygen in the oxidant gas.

The absence of the catalyst poisoning allows the oxidation of the unreacted *p*-NEB after filtering off the *p*-NAP and *p*-NBA sediment. The cooling of the reaction mixture to 0 °C results in crystallisation of most of the *p*-NAP and nearly all of the *p*-NBA. About 13% of the mass of *p*-NAP and ∼10% of the mass of *p*-MNPC remains in the filtrate. To the filtrate is added fresh *p*-NEB until its initial amount is restored together with 30% of the initial amount of $Mn(OAc)_2$ to compensate for its losses with the reaction products. The oxidation is carried out at 140 °C for 4 h. Due to this method

Table 1. **Experiments on *p*-NEB oxidation with recycle**

recycle no.	loaded, g					obtained, g	
	fresh *p*-NEB	filtrate *p*-NEB	filtrate *p*-NAP	filtrate *p*-NMPC	filtrate *p*-NEBHP	*p*-NAP	*p*-NBA
0 (starting run)	77.1					27.0	2.1
1	30.6	36.8	6.3	5.0	0.02	30.3	2.0
2	33.5	36.0	5.9	3.4	0.02	34.5	2.2
8	34.3	35.3	5.5	3.8	0.01	33.7	2.1
9 (filtrate of the 8th recycle)		35.8	5.1	3.4	0.01		
summary load and yield	340.9					295.9	18.9

Table 2. **Quality of the obtained *p*-NAP**

quality indexes	reference sample	washing temperature, °C	
		80	90
basic material content, mass %	96.1	96.1	96.4
melting temperature, °C	79−81	79−80	79−80

of recycling no lowering of the reaction rate is observed even after eight recycles. The results are listed in Table 1.

Altogether there was loaded 340.9 g of *p*-NEB, and there was obtained 295.9 g of *p*-NAP (80% yield) and 18.2 g of *p*-NBA (4.8% yield). Other products are in the filtrate of the last recycle.

The sediment of the raw *p*-NAP obtained by filtration contained 5−8% of the mass of *p*-NEB, 5% of *p*-NBA, and traces of *p*-MNPC. The purification of *p*-NAP was carried out according to the following procedure. The obtained sediment was washed at room temperature by distilled water (150% mass to sediment) to wash out the catalyst. The washed sediment was stirred in 5% solution of Na_2CO_3 at 80−90 °C for 10 min to wash out *p*-NBA. Under these conditions *p*-NAP melted and three-phase system: *p*-NBA sodium salt solution-*p*-NEB-*p*-NAP melt was formed. After settling layers were segregated while still hot. The *p*-NAP melt was poured out into cold water, filtered after crystallisation, and dried until there was a constant mass. The obtained product was pure enough to be used directly for the chloramphenicol synthesis (see Table 2).

The Designing of AP and *p*-NEB Explosion-Proof Oxidation Reactors. The laboratory experiments on AP and *p*-NEB oxidation were carried out in a stirred reactor with a turbine mixer. Such large-scale equipment is complicated, costly, and unserviceable. In designing large-scale gas−liquid reactors the flooded-bubble column is the optimal one. This kind of equipment provides for the high phase contact surface, has simple design and is quite inexpensive. The flow structure in this reactor is best described assuming a continuous stirred tank reactor model for the liquid phase and the plug flow reactor model for the gas phase.

Usually air is the more efficient oxidant than pure oxygen. Thus, its flow should be high enough to provide for the sufficient O_2 concentration and the high reaction rate along the height of the column. At the same time the requirements of the explosion-proof operation limit the O_2 concentration in the outlet flow by few vol %.

Below we present the calculation of the structural dimensions of the flooded-bubble columns. It is assumed that in the AP oxidation the maximum permissible O_2 concentration in the outlet flow should not exceed 3 vol%, and for the *p*-NEB oxidation it can be increased to 7 vol%. The calculation of the AP oxidation column is aimed at the determination of the bubble-layer height that would provide for the safe O_2 concentration in the outlet flow at different column diameters and linear velocities of the oxidant gas. The results of the calculation would allow choosing the column on the cost−performance ratio. The analogous calculation of the bubble-layer height in the *p*-NEB oxidation reactor is at the same time verification for the chosen AP oxidation column. It would be possible to determine whether the predetermined height would provide for the specified maximum permissible O_2 concentration in the outlet flow. Both calculations are based on the link between the O_2 feed rate and the rate of its uptake by the liquid phase.

In the AP oxidation the viscosity of the liquid phase is increasing significantly, so that the operating AP conversion is about 0.4. Under these conditions the term $[Mn^{3+}]K[AP]/[BA]/(1 + K[AP]/[BA])$ in eq 3 is virtually constant[1] and it can be transformed to

$$-\frac{\mathrm{d}[O_2]_g}{\mathrm{d}\tau} = k_{ef}[O_2]_l \qquad (7)$$

where k_{ef} is the rate constant of oxygen uptake in the chemical reaction, min^{-1}, $l[O_2]_g$ is the oxygen concentration in the gas phase, volume fraction, $l[O_2]_g$ is the liquid-phase oxygen concentration, M.

The oxygen mass balance for the adopted flow model on the element height would be as follows:[6]

$$-\frac{\mathrm{d}(w_g[O_2]_g)}{RT\,\mathrm{d}\,H} = k_{ef}[O_2]_l(1-\varphi) \qquad (8)$$

where w_g is the nominal gas velocity in the reactor, m/s, and φ is the aeration factor.

(3) Kuznetsov, M. M.; Obukhova, T. A.; Basaeva, N. N. et al. *Izv. Vuzov. Khim. Khim. Tkhn.* **1980**, *23*, 1220−1224.
(4) Kamneva, A. I.; Koroleva, N. V.; Sinitsina, I. M.; Ryuffer, L. I. *Neftekhimiya* **1982,** *22*, 798−802.
(5) Yoshino, Y.; Hayashi, Y.; Iwahama, T.; Sakaguchi, S.; Ishii, Y. *J. Org. Chem*. **1997**, *62*, 6810−6813.
(6) Gryaznov, I. A.; Digurov, N. G.; Kafarov, V. V.; Makarov, M. G. *Proektirovaniye i Raschet Apparatov Osnovnogo Organicheskogo i Neftekhimicheskogo Sinteza* [*Design and Calculation of the Equipment for the Basic Organic and Petrochemical Synthesis*]; Khimiya: Moscow, 1995.

Table 3. **Explosion-proof height of the batch reactor of benzoic acid manufacture by the AP oxidation**

	reactor height (M) at different values of $\tilde{w}_g$, m/s				
temperature, °C	0.01	0.03	0.05	0.07	0.09
130	4.3	5.2	6.2	7.1	8.0
140	3.5	4.1	4.7	5.7	6.0
150	2.9	3.3	3.8	4.2	4.6

For the low-soluble gases $[O_2]_l = [O_2]_g/\gamma$, and assuming the average nominal velocity $\tilde{w}_g$ constant along the reactor height integrating eq 8 obtains

$$[O_2]_g^{out} = [O_2]_g^{in} \exp\left[-\frac{(1-\varphi)k_{ef}HRT}{\tilde{w}_g\gamma}\right] \quad (9)$$

where $[O_2]_g^{out}$ and $[O_2]_g^{in}$ are the oxygen concentrations at the reactor outlet and inlet respectively, volume fraction; γ is the oxygen solubility coefficient; H is the height of froth (aerated mass) in the reactor, m; and $\tilde{w}_g$ is the gas average nominal velocity, m/s.

If the reaction proceeds in the diffusion or transition region, then the rate constant of the chemical reaction, k_{ef} is changed for rate constant of oxygen uptake equal to

$$k_{O_2} = \frac{1}{\frac{1}{k_{ef}} + \frac{1}{\beta f}} \quad (10)$$

where β is the mass-transfer coefficient, and f is the specific area of phase contact that is proportional to gas velocity in a wide range.[7]

If the reactor temperature is constant, then

$$\beta f = k_S\tilde{w}_g \quad (11)$$

where k_S is the proportionality coefficient linking the area of phase contact with the gas velocity, m^{-1}.

Substituting of the defined values of $[O_2]_g^{out}$ and $\tilde{w}_g$ into eq 9 and transforming it, one obtains the height of froth (aerated mass) in the reactor

$$H = \frac{\gamma\tilde{w}_g}{RT(1-\varphi)}\left(\frac{1}{k_{ef}} + \frac{1}{k_S\tilde{w}_g}\right)\ln\frac{[O_2]_g^{in}}{[O_2]_g^{out}} \quad (12)$$

Equation 12 can be simplified if $k_{ef} \gg k_S\tilde{w}_g$, i.e., the process rate is limited by the oxygen diffusion rate

$$H = \frac{\gamma}{RT(1-\varphi)k_S}\ln\frac{[O_2]_g^{in}}{[O_2]_g^{out}} \quad (13)$$

The values of the froth (aerated mass) heights in the column that provide the safe outlet oxygen concentration of 3 vol % in the gas phase are listed in Table 3. The values were calculated according to eqs 12 and 13 for the reaction temperatures 130, 140, and 150 °C and nominal gas velocities 0.01−0.09 m/s. The experimental rate constant values at the initial $Mn(OAc)_2$ concentration 0.05 M are

$$k_{ef} = (1.2 \times 10^8)\exp(-7220/T), \quad c^{-1}$$

$$k_S = (4.12 \times 10^5)(-3900/T), \quad m^{-1}$$

$$\gamma = (1.99 \times 10^4)\exp(-1070/T), \quad L\ atm\ mol^{-1}$$

The choice of the particular reaction conditions, reactor dimensions, and the nominal velocity $\tilde{w}_g$ is determined by the results of the cost−performance calculation. Thus, the increase in the oxidant gas velocity would increase the entrainment of the reaction mixture vapours that in turn results in the growth of the heat transfer area and the complication of the condenser equipment. On the other hand, the low $\tilde{w}_g$ value decreases the mass transfer area and impairs heat transfer conditions. That is especially significant for the fast exothermal reactions with the high heat of reaction.

According to eq 3 the rate of *p*-NEB oxidation depends both on the oxygen content in the oxidant gas and on the substrate concentration in the liquid phase. This concentration under batch conditions is decreased during the reaction from 7.0 to 4.9 M. The initial concentration value is lower than the theoretical one (7.4 M) due to the dilution of the substrate by the recycled reaction products. The tower diameter that secures the desired capacity is 0.4 m. The flooded section height at $\varphi = 0$ is 3.82 m. The target of the present calculation is to determine whether this height value will secure that the oxygen outlet concentration would not exceed 7 vol % both at the beginning and at the end of the process at the constant air flow.

Assuming that the inlet and outlet oxygen concentrations are 21 and 3 vol %, respectively, we obtain the average oxygen concentration in the oxidant gas at the beginning of the reaction at [*p*-NEB] = 7.0 M:

$$[\tilde{O}_2]_g = \frac{[O_2]_g^{in} - [O_2]_g^{out}}{\ln([O_2]_g^{in}/[O_2]_g^{out})} = 2.73 \times 10^{-3}\ mol/L \quad (14)$$

The reaction rate calculated according to the eq 3 is

$$-\frac{d[p\text{-NEB}]}{d\tau} = (3.42 \times 10^{-2})7.0\sqrt{2.73 \times 10^{-3}} = 1.25 \times 10^{-2} mol\ L^{-1}\ min^{-1}$$

where $3.42 \times 10^{-2}\ min^{-1}\ M^{-1/2}$ is the effective rate constant at 140 °C and $[Mn(OAc)_2]_0 = 0.025$ M.

The oxygen flow calculated on the reactor volume $G_{O_2} = 0.1024\ mol\ s^{-1}$. Then the air flow at the beginning of the reaction under standard conditions is

$$G_{air} = G_{O_2}\frac{1-0.03}{0.21-0.03} = 0.552\ mol\ s^{-1} = 44.5\ m^3\ h^{-1}$$

Let us assume that at the end of the process the outlet oxygen concentration is 7 vol % due to the decrease in the *p*-NEB concentration to 4.9 M and corresponding decrease in the oxygen uptake rate (according to eq 3). This concentration secures the explosion-proof reaction conditions. The average oxygen concentration in the oxidant gas at [*p*-NEB] = 4.9 M is $[\tilde{O}_2]_g = 3.76 \times 10^{-3}$ M and the reaction rate is

(7) Levenspiel, O. *Chemical Reaction Engineering*; John Wiley: New York, 1965.

$$-\frac{\mathrm{d}[p\text{-NEB}]}{\mathrm{d}\tau} = (3.42 \times 10^{-2})4.9 \cdot \sqrt{3.76 \times 10^{-3}} = 1.03 \times 10^{-2}\ \mathrm{mol\ L^{-1}\ min^{-1}}$$

and the oxygen flow is $G_{O_2} = 0.0841$ mol s^{-1}.

Then the air flow under standard conditions is

$$G_{air} = 0.084\frac{1 - 0.07}{0.21 - 0.07} = 0.559\ \mathrm{mol\ s^{-1}} = 45\ \mathrm{m^3\ h^{-1}}$$

Thus, the constant air volume velocity of 45 m^3 h^{-1} secures the explosion-proof conditions both with the high oxygen uptake rate at the beginning of the process and with the low one at the end.

The necessary flooded height at the beginning and at the end of the process was calculated by eq 15 analogous to eq 8

$$-\frac{\mathrm{d}(\tilde{w}_g[\mathrm{O_2}]_g)}{\mathrm{d}H} = k_{\mathrm{ef}}[p\text{-NEB}]\sqrt{[\mathrm{O_2}]_g} \qquad (15)$$

The nominal air velocity at 140 °C is

$$\tilde{w}_g = \frac{G_{air}T}{T_0 S} = 0.15\ \mathrm{m\ s^{-1}} \qquad (16)$$

where $T = 413$ K, $T_0 = 273$ K, and $S = 0.126$ m^2 is the column cross sectional area.

Integrating eq 15 obtains

$$H = 2\frac{([\mathrm{O_2}]_g^{\mathrm{in}})^{1/2} - ([\mathrm{O_2}]_g^{\mathrm{out}})^{1/2}}{k_{ef}[p\text{-NEB}]}\tilde{w}_g \qquad (17)$$

At [p-NEB] = 7.0 M, $[\mathrm{O_2}]_g^{\mathrm{in}} = 21$ vol % and $[\mathrm{O_2}]_g^{\mathrm{out}} = 3$ vol % the flooded height H is 3.65 m; at [p-NEB] = 4.9 M, $[\mathrm{O_2}]_g^{\mathrm{in}} = 21$ vol % and $[\mathrm{O_2}]_g^{\mathrm{out}} = 7$ vol % it is 3.59 m. Thus, it is evident that the adopted value of the flooded height secures the desired final outlet oxygen concentration.

The above examples demonstrate the application of the results of the heterogeneous kinetics study to the design of the large-scale reactors.

Acknowledgment

The authors thank Dr. Felix Sirovski for the valuable help in the preparation of the paper.

Received for review April 13, 1999.

OP990030Q